Remote Sensing in Ecology and Conservation
Open Access
ZSL

RESEARCH ARTICLE

Modelling forest dynamics using integral projection models and repeat lidar

Alice Rosen[1], Robin Battison[2], Christina M. Hernández[1], Oliver G. Spacey[1], Jessica McLean[1], Suzanne M. Prober[3], Samuel J. L. Gascoigne[1,4], Sean McMahon[5,6], Tommaso Jucker[2] & Roberto Salguero-Gómez[1]

[1]Department of Biology, University of Oxford, South Parks Road, Oxford OX1 3EL, UK
[2]School of Biological Sciences, University of Bristol, 24 Tyndall Avenue, Bristol BS8 1TQ, UK
[3]CSIRO Environment, Canberra ACT, 2601, Australia
[4]School of Biological Sciences, University of Aberdeen, Aberdeen AB24 2TZ, UK
[5]Smithsonian Environmental Research Center, 647 Contees Wharf Road, Edgewater MD, 21037-0028, USA
[6]Forest Global Earth Observatory, Smithsonian Tropical Research Institute, Panama City, Panama

Keywords
airborne laser scanning (ALS or lidar), demography, drought, forest dynamics, Integral Projection Model (IPM), remote sensing

Correspondence
Alice Rosen, Department of Biology, University of Oxford, South Parks Road, Oxford, OX1 3EL, UK. E-mail: alice.rosen@biology.ox.ac.uk. Telephone: +01865 275000

Funding information
AR was supported by the Oxford BBSRC Doctoral Training Partnership (BB/T008784/1). CMH and RSG were supported by an NERC Pushing the Frontiers grant to RSG (NE/X013766/1). CMH was additionally supported by a Marie Curie Fellowship (MSCA DensPopDy #10115386) with funding through UKRI (EP/Z002826/1). OGS was supported by the Oxford NERC Doctoral Training Partnership (NE/S007474/1). TJ was supported by a UK NERC Independent Research Fellowship (NE/S01537X/1) and by a UKRI Frontier Research grant (EP/Y003810/1) that also funded RB.

Editor: Prof. Mat Disney
Associate Editor: Dr. Gaia Vaglio Laurin

Received: 23 May 2025; Revised: 21 October 2025; Accepted: 25 November 2025

doi: 10.1002/rse2.70050

Abstract

Estimating tree life histories and population dynamics is key to predicting how forests respond to climate change and disturbance. However, linking individual tree trajectories to whole-forest outcomes (e.g. structural, compositional, and functional health) remains challenging. Stage-structured demographic models offer a promising solution, but they typically require extensive field data on individual-level vital rates (e.g. survival and growth), limiting their application at scale. Here, we demonstrate an approach that integrates repeat airborne lidar data with a structured demographic model (an integral projection model, IPM) to examine forest-wide demography in response to environmental drivers. Using Australia's Great Western Woodlands as a case study, we model the survival, growth, and life expectancy of ~40 000 eucalypt trees over a decade. Vital rates were modelled using height for small trees and crown area for large trees, reflecting a shift in growth strategy with size. Our results indicate distinct responses of small and large trees to proxies for competition and soil moisture (local canopy density and topographic wetness index, respectively). A reduction in topographic wetness index—reflecting drier conditions—led to lower life expectancy, particularly for larger trees, which may be more vulnerable to drought. This framework enables demographic analysis at scale, using widely available lidar data, offering a scalable tool for forest monitoring, modelling, and management. We identify three priorities for broader application, including (1) mixed species stands and multilayered canopies, (2) full life cycle modelling including reproduction and early life stages, and (3) long-term or comparative studies using high-quality repeat lidar. By combining remote sensing data with detailed insights from field-based studies, our study provides a scalable approach for guiding forest management and conservation decisions.

Introduction

The world's forests are facing growing pressure from climate change and land-use intensification, with major implications for carbon and water cycling, biodiversity, and people (McDowell et al., 2020; Seidl & Turner, 2022). However, projecting how forests will respond to these changes is inherently challenging due to the vast spatial and temporal scales at which forests operate. In response, a wide range of modelling approaches have been applied to understand and predict the impact of these threats (Decocq et al., 2023). Models that incorporate demography have become of particular importance due to the advantage of including individual dynamics in the assessment of community, landscape, or biome-scale properties (Merow et al., 2014).

Demographic models, which parameterize and simulate vital rate processes such as survival, growth, and reproduction, allow us to quantify the varied life history strategies of trees and produce metrics that capture long term or large-scale features of populations, such as generation time, mean life expectancy, and time to size (Clark & Clark, 1992; Needham et al., 2022). These models therefore allow us to examine how specific threats may disproportionately impact certain size classes or stages. For example, drought strongly impacts the growth of the largest trees (Bennett et al., 2015; Trouillier et al., 2019), while selective logging of mature trees may lead to regeneration failure (Bartholomew et al., 2024).

Demographic approaches are, however, data hungry (Doak et al., 2005; Ramula et al., 2009), requiring data on the vital rates for hundreds—if not thousands—of individuals in the population of interest. For long-lived trees, it is rarely possible to observe an individual across the potential lifespan. Instead, vital rates can be estimated by monitoring individuals in a population at two or more time points. Still, producing robust estimates of vital rates is easier said than done. In particular, obtaining data on tree vital rates at the beginning (i.e. reproduction/recruitment; Bogdziewicz et al., 2024) and end of their life cycle (i.e. adult mortality; McMahon et al., 2019) is challenging (Ruiz-Benito et al., 2020).

Growth data are most commonly estimated from repeated measurements of diameter at breast height (DBH) of the tree stem (Lines et al., 2022). This change in diameter can be related to other features of productivity, such as basal area change or change in aboveground biomass, using allometric equations designed for these applications (e.g. Chave et al., 2014). These allometries, however, are known to be gross simplifications of how trees actually invest in structure and how those structures might change over time (e.g. investment in vertical and lateral crown expansion; Pretzsch et al., 2013). Moreover, most tree demographic data come from plots that represent relatively small samples of the forests in which they are established. Remote sensing offers ways of inferring features of forest demography over much larger spatial scales.

Light detection and ranging (lidar) in particular has improved how forest structure and change are observed over landscapes, regions and now globally (Dubayah et al., 2022). Lidar sensors emit high frequency laser pulses and measure the time it takes for those pulses to return to the sensor. Mounted on an airplane or unoccupied aerial vehicle (UAV), lidar therefore allows us to capture the 3D structure of forest canopies at scale, in the form of a detailed point cloud model (Camarretta et al., 2020). From a point cloud, many of the features of structure formerly estimated with bias and error from DBH allometries can be inferred in more detail. This technology also provides a change in perspective towards the canopy, where biologically relevant processes and dynamics take place (Lines et al., 2022). Furthermore, lidar data are becoming more widely and freely available (Beland et al., 2019; Fischer et al., 2025), offering the opportunity to extend the application of demographic modelling approaches across broader scales and forest types. Despite the quantity of remote sensing data now being generated, and an uptake in the use of lidar data by ecologists in recent years, these datasets remain under-utilized in demographic modelling.

Here, we introduce a pipeline for combining remote-sensing data with a structured demographic model to demonstrate their potential for elucidating forest dynamics at scale. As a case study, we model the demographic changes of $\sim$40 000 eucalypt trees in a fast-drying region of south-western Australia (CSIRO, 2022). We assess how the survival, growth, and remaining life expectancy of individuals in this population are affected by different biotic (canopy density) and abiotic conditions (soil moisture). Then, we discuss the advantages and limitations of a remote-sensing approach to forest demographic modelling. Finally, we highlight three areas of future research that are key to broadening the application of this framework: to more complex systems (e.g. mixed species stands and dense, multilayered canopies), across complete life histories (e.g. to include reproduction and early life stages), and for long-term or comparative studies (e.g. through improved availability of high-quality, repeat lidar surveys and integration with field data).

Materials and Methods

Here, we use a case study to demonstrate the pipeline for parameterizing an integral projection model (IPM) using remotely sensed data (Fig. 1). The pipeline broadly

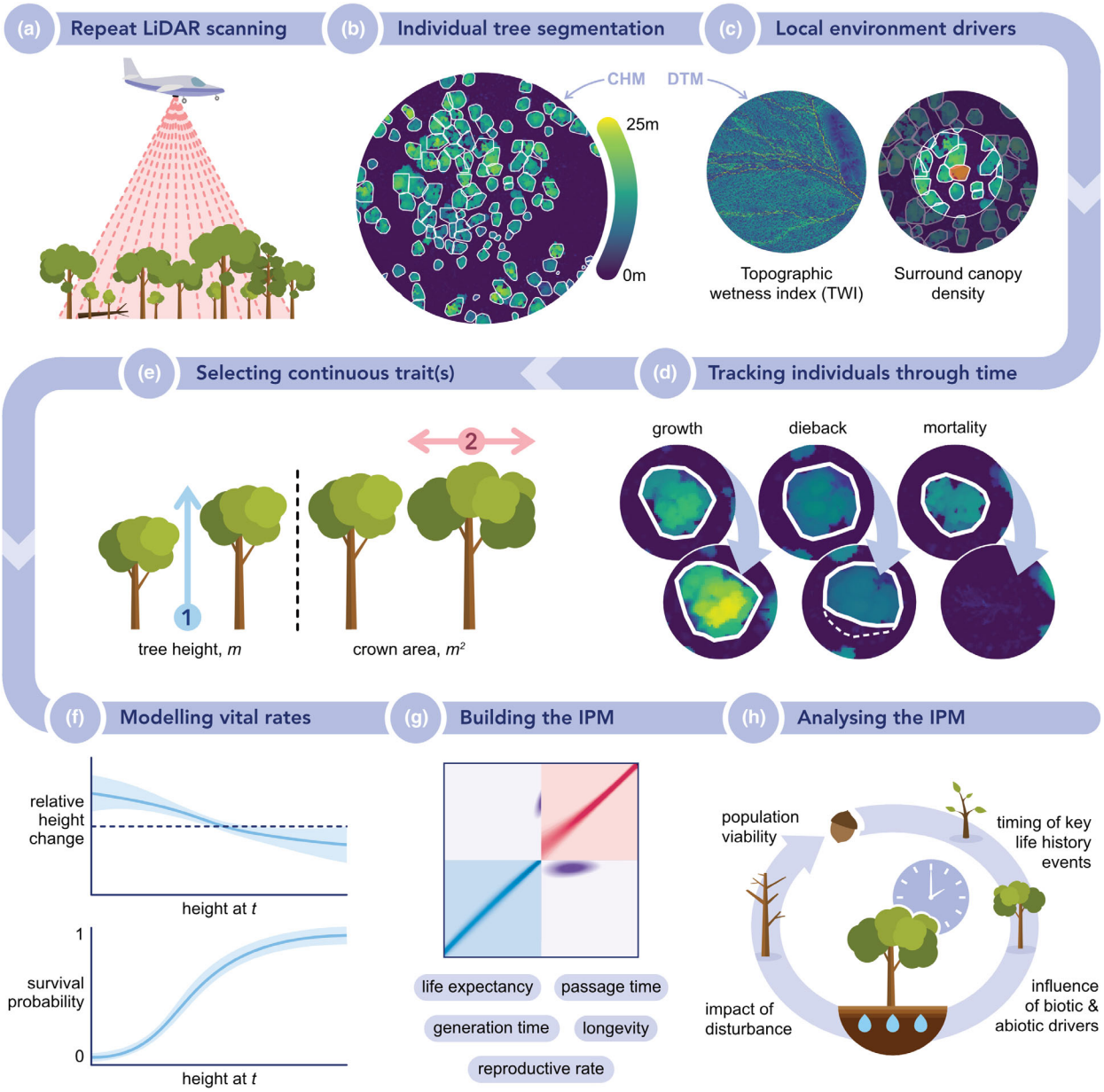

Figure 1. Pipeline for integrating lidar data with structured demographic models for ecological inference. (a) Forest populations are surveyed at appropriate time intervals with a lidar scanner to produce high-resolution 3D point clouds. Point clouds are processed into canopy height models (CHMs) and digital terrain models (DTMs). (b) Individual tree segmentation is performed using a CHM-based algorithm (e.g. Dalponte & Coomes, 2016). (c) Relevant environmental variables are derived. For example, TWI is an indicator of soil moisture accumulation (Kopecký et al., 2021) and is calculated from the DTM. Local competition is inferred from the canopy density surrounding each tree, using the CHM. (d) Trees are matched across time points using a crown-matching algorithm (Battison et al., 2024; Olsoy et al., 2024), before measuring changes in size and classifying mortalities. (e) Continuous traits (e.g. height and crown area) are evaluated for their ability to predict survival and growth across the life cycle. (f) Selected traits and environmental parameters are used to model the vital rates using regressions. (g) The integral projection model (IPM) is constructed based on the selected vital rate models and key life history traits (e.g. mean life expectancy, longevity, generation time) are calculated. (h) Finally, IPM outputs are analysed to test ecological hypotheses.

involves five key steps: (1) using repeat lidar data to track individuals through time; (2) selecting relevant traits (e.g. tree height and crown area) for predicting vital rates; (3) modelling vital rates from the selected traits, as well as relevant lidar-derived environmental drivers; (4) building a multistage IPM that captures the primary (height) and

secondary (crown expansion) growth of these trees and (5) analysing the IPM to understand the relative influence of biotic (e.g. density dependence) and abiotic drivers (e.g. soil moisture) on key emerging properties of the population model, such as life expectancy.

Case study: Eucalypt woodlands of southwestern Australia

Study site and species

The Great Western Woodlands Terrestrial Ecosystem Research Network (TERN) SuperSite is in southwestern Australia (30°11′S, 120°39′E, 430–475 m a.s.l). The Great Western Woodlands is a semi-arid region, comprising one of the largest intact temperate woodlands in the world (Watson et al., 2008). Increasingly warm, dry conditions in the region are driving more frequent droughts and wildfires (CSIRO, 2022; Peters et al., 2021; Prober et al., 2012). The 25 km^2 study site at the core of the SuperSite is predominantly old-growth woodland that has remained undisturbed by fire for centuries. The site is largely dominated by four obligate-seeding eucalyptus species: *Eucalyptus salmonophloia* (the most abundant), as well as *E. salubris*, *E. transcontinentalis*, and *E. clelandiorum* (Gosper et al., 2018). In its old-growth phase, the woodland features a relatively sparse, open canopy of large, single-stemmed trees. The dominant species can reach 10–25 m in height and can live to over 400 years (Jucker et al., 2023). Mulga scrub (*Acacia* sp.) and heathland occur in small mosaics with the eucalypt woodlands, but cover $<0.1\%$ of the study site and were excluded from our analyses.

Lidar data

Airborne lidar data were acquired in May 2012 and May 2021 across our 5×5 km^2 study site, producing a 3D 'point cloud' of the woodland. The 2012 lidar survey was conducted by Airborne Research Australia (https://www.airborneresearch.org.au) using a motorized glider (Diamond Aircraft, HK36 TTC-ECO) flown at 300 m altitude and mounted with a RIEGL LMS-Q560 scanner. The 2021 data were collected by Aerometrex (https://aerometrex.com.au) using a fixed wing aircraft (Cessna 404 Titan), flown at 1100 m altitude and mounted with a REIGL VQ-780ii scanner. Both surveys achieved similar high pulse densities, despite differences in the acquisition parameters and instrumentation (21.4 and 23.6 m^{-2} for the 2012 and 2021 surveys, respectively).

From these high-quality 3D point clouds, we generated 2D maps of canopy height, known as canopy height models (CHMs; Fischer et al., 2024). The georeferenced point clouds for both lidar surveys were processed using a combination of CloudCompare (https://danielgm.net/cc), QGIS (https://qgis.org) and R version 4.1.0 (R Core Team, 2021). See Supporting Information for details. We used the pit-free algorithm in the *lidR* R package (Khosravipour et al., 2014) to produce a 0.5 m resolution normalized CHM and a 5 m resolution digital terrain model (DTM). We selected this algorithm to optimize comparability between the two surveys, as it is robust when applied to high-quality point clouds (Fischer et al., 2024; Zhang et al., 2024). All subsequent data processing and analyses were conducted in R version 4.1.0.

Using lidar to track individuals through time

Individual tree segmentation and crown matching

To estimate individual tree survival and growth, we segmented tree crowns from the CHMs using the widely applied *dalponte2016* algorithm (Dalponte & Coomes, 2016), following the process outlined by Battison et al. (2024). Briefly, this algorithm applies a local maximum filter within a moving window to locate treetops and delineate crowns based on height-crown area allometries. We calibrated window size using a manually delineated subset of trees ($n = 797$). For this subset, Battison et al. (2024) reported an overall segmentation accuracy of 82% and an over-segmentation rate of 5%. Alternatively, databases such as Tallo (Jucker et al., 2022) can inform allometric relationships. CHM-based algorithms (in contrast to those that work on the underlying point cloud) are computationally cheaper and generally more robust to differences in how the data are acquired (Fischer et al., 2024; Mielcarek et al., 2018).

To track individuals across time, we matched crowns between the 2012 and 2021 surveys using the approach developed by Battison et al. (2024). Crowns were retained if a single 2021 centroid fell within the 2012 crown boundary. This step aimed to minimize over-segmentation and spurious size changes between the two time points. To exclude small shrubs from our analysis we removed crowns <3 m in height or <9 m^2 area. The outcome of this filtering process was a subset of time-matched eucalypt tree crowns ($n = 39\,286$) that we used to model tree growth in the construction of the IPM.

Local environment drivers

We used two lidar-derived variables to assess the biotic and abiotic drivers of tree vital rates. Neighbourhood canopy density (a proxy for competition; Vanderwel et al., 2020) was calculated as the mean CHM height

(in 2012) within a 25 m radius of the perimeter of each tree crown (Battison et al., 2024; Zhao et al., 2006). Topographic wetness index (TWI; Kopecký et al., 2021), a proxy for local soil moisture and nutrient availability, was calculated from the 5 m DTM using the *dynatopmodel* R package (Metcalfe et al., 2015) and assigned to trees based on their coordinates. The 5 m raster resolution captures hillslope water convergence while reducing noise from microtopographic variation.

Estimating vital rates from lidar

Selecting relevant traits for vital rate modelling

We assessed which lidar-derived size metrics best captured tree vital rates (survival and growth): tree height, crown area, and their product ('tree size'). Tree height was calculated as the mean canopy height within each delineated tree crown, which is less sensitive to outliers (e.g. clouds, birds) than the maximum value. In our data, mean and maximum height were highly correlated ($R^2 = 0.87$; $P < 0.001$). Crown area was defined as the area of the tree crown polygon. Both traits were calculated using the *terra* package in R (Hijmans, 2024). Growth patterns varied with tree size: smaller trees prioritized height growth, while larger trees expanded their crowns, a common strategy among trees (Fig. S1; King, 2011, Franceschini et al., 2016).

To capture the two growth strategies, we modelled vital rates separately for small and large trees. We used a 7.27 m height threshold—where relative height and crown growth were equal (Fig. S2)—to distinguish between small ('minor class') and large ('major class') individuals. This threshold was close to the 2012 median tree height (7.06 m). Trees below this threshold in both years were assigned to the minor class, whereas trees above the threshold in both years were assigned to the major class (Fig. 2a). Additionally, we modelled the growth of trees that transitioned over the threshold between surveys ('promotion') and those that fell below it ('demotion'). Vital rates were modelled using log-transformed height

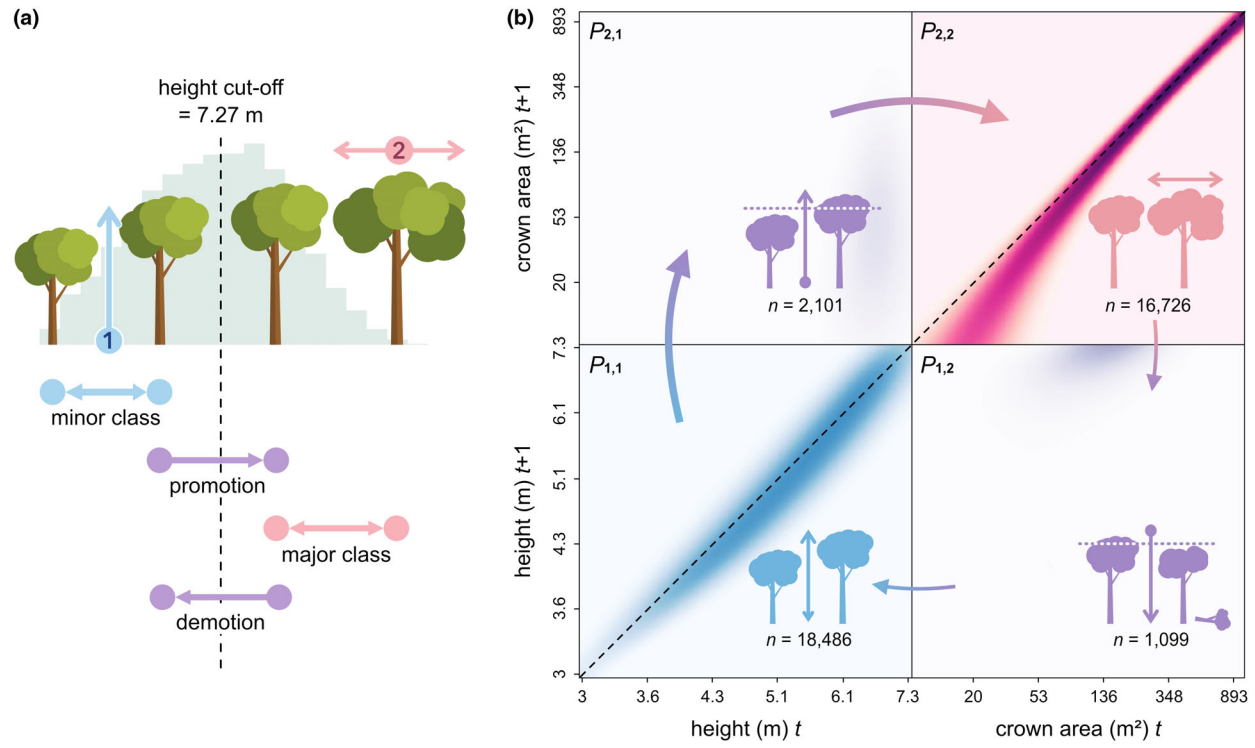

Figure 2. Two-stage integral projection model (IPM) for eucalypt population dynamics. (a) Trees were assigned to a class based on their size at time t and $t+1$, relative to a height threshold of 7.27 m. (b) The P-kernel (survival [Equation 1] and growth [Equation 2] component of an IPM) shows the probability of a tree of size x at time t surviving and growing to be size y at $t+1$, with colour intensity indicating probability. Cell $P_{1,1}$ (blue) represents minor class trees (height-based), $P_{2,2}$ (pink) represents major class trees (crown area) and $P_{2,1}$ and $P_{1,2}$ (purple) represent transitions between the two main classes—promotion (minor to major) and demotion (major to minor). The clockwise arrows represent the theoretical transition of a tree through its lifetime as it grows, surpasses the height cut-off and then shrinks again—perhaps due to dieback or damage from storms.

for minor class trees and log-transformed crown area for major class trees.

Modelling survival and growth

To predict vital rates across size classes, we compared a set of ecologically meaningful models. Selection of the best-supported model was based on a combination of the Akaike information criterion and our biological knowledge of the system (Table S1).

To model the survival of individual trees, we first classified mortality events via a two-step process. First, for matched crowns ($n = 39\,286$; Using lidar to track individuals through time Section), trees with $> 30\%$ reductions in height and/or crown area were classified as dead, following Duncanson and Dubayah (2018) and Ma et al. (2023). Second, to capture mortality events where crowns could no longer be detected in the second survey, we overlaid 2012 crowns onto the 2021 CHM and applied the same $> 30\%$ reduction threshold for height loss. We performed a sensitivity analysis to examine how the choice of percentage threshold shapes mortality rates (Fig. S5).

We modelled the probability that an individual tree survives from time t (2012) to $t+1$ (2021), given its size at time t, using logistic regressions. The selected model for both minor and major classes was

$$\text{logit}(s(z)) = \beta_o + \beta_z \times z + \beta_{z^2} \times z^2 + \beta_{\text{TWI}} \times \log(\text{TWI}) + \beta_{\text{CD}} \times \log(\text{CD}), \quad (1)$$

where z is the log-transformed size of an individual at time t, TWI is topographic wetness index, CD is canopy density, and the β's are the fitted coefficients. The probability of survival ($s(z)$) only depends on size at time t, regardless of whether individuals remain in the same class or promote/demote to another (Fig. 2).

Growth was modelled as the change in tree height or crown area between 2012 and 2021 using the 39 286 matched tree crowns (Fig. 1). For each size class, we modelled the expected tree size distribution at time $t+1$ for an individual of size z at time t, conditional on having survived from time t to $t+1$. All growth models included quadratic terms (except for demotion, which used a linear function; Table S1):

$$z' = \beta_o + \beta_z \times z + \beta_{z^2} \times z^2 + \beta_{\text{TWI}} \times \log(\text{TWI}) + \beta_{\text{CD}} \times \log(\text{CD}), \quad (2)$$

where z' is the log-transformed size at $t+1$, and all other variables are as previously defined. To account for variation in individual growth trajectories, we estimated the size dependence of this variance by regressing the residuals in the growth model against size at time t (Table S1).

We assessed model accuracy using discrimination and calibration metrics for survival models (AUC, Brier score, and Tjur's R^2) and R^2 and RMSE for growth models (Table S2), with residual diagnostics shown in Fig. S4.

Building the IPM

IPMs (Coulson, 2012; Easterling et al., 2000; Merow et al., 2014) examine how continuous traits of individuals (e.g. size) relate to vital rates of survival, growth, and reproduction. By using one or more continuous traits (Zambrano & Salguero-Gómez, 2014), an IPM allows us to create population projections that identify the individuals most at risk from threats such as climate change and the impact on populations as a whole (Laurans et al., 2024; Ohse et al., 2023).

We parameterized an IPM using the vital rate equations described above. In this case study, we focus on the survival and growth of the existing population under different conditions of canopy density and soil moisture. The component of an IPM that captures the survival and growth transitions of an existing population (without reproduction) is known as the P-kernel:

$$P(z', z) = s(z)g(z', z), \quad (3)$$

where $s(z)$ is the survival probability for an individual of size z at time t (Equation 1), and $g(z', z)$ is the growth function describing the probability density of size z' at time $t+1$, given an individual's size z at time t, conditional on having survived (Equation 2). We note that to model the reproductive component (typically referred to as the $F(y, x)$ kernel), one would also need data on fecundity rates and establishment probabilities (e.g. Easterling et al., 2000). See applications of our framework to systems with reproductive data in Completing the life cycle section.

Constructing a two-stage IPM

To account for the changing growth trajectory of eucalypt individuals—from height growth to crown expansion—we constructed a two-stage P-kernel using a 2×2 mega-matrix $\boldsymbol{M}$ (Goodman, 1968; Zambrano & Salguero-Gómez, 2014). Each of the four blocks in the mega-matrix (Fig. 2) contains vital rates as functions of continuous traits (height and/or crown area): $P_{1,1}$, survival and growth of minor class individuals (based on height) remaining in the minor class; $P_{2,1}$, promotion

from the minor class (height) to the major class (crown area); $P_{2,2}$, survival and growth of major class individuals (crown area) remaining in the major class, and $P_{1,2}$, die-back from major (crown area) to minor (height) class.

Reproduction (the *F*-kernel described above) can also be accommodated in the cell $\boldsymbol{M}_{1,2}$, together with $P_{1,2}$. We modified the above *P*-kernel to include the probability that an individual of size z at time t remains in the same class at $t+1$ (rather than being promoted or demoted from the current size class):

$$P(z', z) = s(z)g(z', z)r(z), \tag{4}$$

where $r(z)$ is the probability of remaining in the same size class. We modelled this probability using a generalized linear model with logit link function:

$$\begin{aligned}\text{logit}(r(z)) = {} & \beta_o + \beta_z \times z + \beta_{z^2} \times z^2 + \beta_{\text{TWI}} \times \log(\text{TWI}) \\ & + \beta_{\text{CD}} \times \log(\text{CD}).\end{aligned} \tag{5}$$

IPMs require careful handling of survival and growth predictions to avoid issues such as 'eviction', where individuals are artificially removed from the model (see Supporting Information; Merow et al., 2014). Here, we corrected for eviction in all but the major class kernel, where we instead retained the natural reduction in survival of the largest trees to avoid unrealistic population projections.

Analysing the IPM

A variety of life history traits that inform on the vitality and trajectory of a population can be easily calculated from IPMs (Salguero-Gómez et al., 2016). Some of these traits can be directly derived with only survival and growth information from the *P*-kernel (Zambrano & Salguero-Gómez, 2014). Here, we used the *Rage* package (Jones et al., 2022) to estimate remaining life expectancy —the average number of additional years an individual of a given size is expected to live. Life expectancy has a direct impact on population biomass (Needham et al., 2022) as well as being a proxy for carbon capture and storage because large, long-lived trees will capture and retain more carbon over their lifetimes than shorter-lived species.

We calculated life expectancy across the full size distribution, from the smallest trees—3 m height or 9 m^2 crown area—up to the largest observed individuals. To explore how a/biotic drivers shape demographic responses, we perturbed canopy density and TWI values by ±50% of their standard deviation, relative to the site mean. We then fit a linear model that included interactions between size class (minor or major), perturbation level (mean value, ±50%), and the perturbed variable (TWI or canopy density). We also visually compared model predictions to the full range of possible life expectancy outcomes under different conditions of TWI and canopy density, up to the most extreme values observed for this population (Fig. 3).

Finally, we provide an example of an elasticity analysis (Griffith, 2017), which assesses the relative contribution of vital rate parameters (Equations 1 and 2) to a life history trait of interest—in this case, mean life expectancy of the smallest individuals. The elasticity analysis reveals the demographic pathways through which TWI and canopy density may be driving a change in life expectancy (Easterling et al., 2000). For example, a decline in life expectancy could result from reduced survival of small trees, or an absolute reduction in growth across size classes (Fig. 4).

Results

We modelled the demographic changes of 42 213 eucalypt trees using an IPM parameterized with repeat lidar data. The survival, growth and remain-in-class models used to construct the IPM showed reasonable predictive accuracy (Table S2). Calibration and residual diagnostics indicate generally good model fit, with no major violation of assumptions; the main exception being some miscalibration at probability extremes for major class survival, likely due to large tree mortality being a rare event (Fig. S4).

We assessed the contribution of TWI and canopy density to the life expectancy of trees across size classes. Life expectancy was strongly linked to tree size, with trees at intermediate sizes (5.5–7.4 m in height and 8.9–220 m^2 in crown area) predicted to have the highest number of additional years left to live (118 years on average; Fig. 3). Overall, large trees (those in the major class; Fig. 2a) had a higher life expectancy (105 years) compared to smaller trees (minor class; 73 years), under average conditions of TWI and canopy density.

Changes in TWI (±50% of SD) had a greater impact on life expectancy than changes in canopy density. A 50% increase in TWI extended life expectancy by 26 years for major class trees ($P < 0.001$; Fig. 3a) and by 18 years for minor class trees ($P = 0.235$). Conversely, a 50% decrease in TWI led to a pronounced reduction in life expectancy, particularly for major class trees (−25 years; $P < 0.001$), while the reduction for minor class trees (−17 years) was not statistically significant ($P = 0.265$). In contrast, changes in canopy density had a smaller effect. A 50% reduction in canopy density had a slight positive impact (Fig. 3b), increasing life expectancy by 7 years for both major class ($P = 0.036$) and minor class trees ($P = 0.585$).

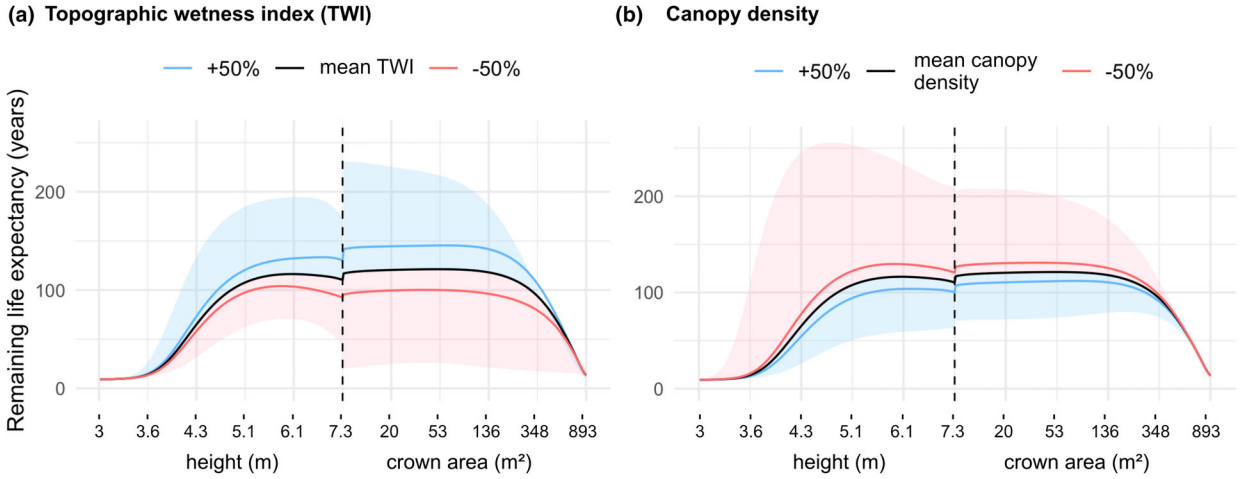

Figure 3. Effect of topographic wetness index (TWI) and canopy density on remaining life expectancy across tree sizes. The vertical dashed line separates minor (left) and major (right) size classes. The black line represents life expectancy under mean conditions of TWI and canopy density observed in the 25 km^2 study site. Blue and red lines show life expectancy changes when TWI (a) or canopy density (b) are increased (blue) or decreased (red) by ±50% of the variable's SD. The perturbations are therefore scaled to reflect typical variability in TWI and canopy density. Shaded regions show the range of possible life expectancies under different conditions of TWI/canopy density, with upper and lower bounds representing the most extreme observed values in the study site. Life expectancy increased with TWI, particularly for large trees, but declined slightly as canopy density increased.

The elasticity analysis (Fig. 4) confirmed that the life expectancy of small trees is more sensitive to changes in TWI than to changes in canopy density. The same pattern was observed for large trees (Fig. S7). Increasing TWI had a generally positive impact on life expectancy, primarily by improving the survival probability of minor class trees (Fig. 4c)—the most 'elastic' vital rate parameter (Fig. 4b). In contrast, increasing canopy density had a weaker negative effect by lowering the survival of minor class trees over 5.15 m tall (Fig. 4d).

Discussion

While field-based monitoring campaigns provide detailed insights into tree demography (Needham et al., 2018), they are limited to relatively small spatial scales. To improve predictive models, policy initiatives, and ecosystem-scale understanding, forest change must be quantified at broader landscape and regional scales. In this study, we introduced a scalable pipeline that uses repeat lidar to parameterize a demographic model, applied here to Australia's Great Western Woodlands.

Our analysis of over 40 000 trees revealed clear size- and environment-driven patterns in life expectancy. On average, large trees had a higher life expectancy than small trees. This pattern arises because IPMs estimate the mean fate of individuals. Since mortality is high at small sizes (e.g. due to clustering and potential thinning; Fig. S6), the average life expectancy of smaller trees is lower—even though a subset will survive and grow into large, long-lived individuals. TWI emerged as a much stronger driver of life expectancy than canopy density, indicating that soil moisture availability governs both growth and survival more than crowding in this semi-arid eucalypt woodland. Large trees were particularly sensitive to TWI (Fig. 3); while their deeper root systems and higher carbon reserves may support survival in typical years, larger trees of many species are more vulnerable to drought due to greater inherent hydraulic stress (Bennett et al., 2015; Trouillier et al., 2019). Yates et al. (2000) found that mature *E. salmonophloia* (the most abundant species in the study site) strongly competes for limited soil water, suppressing seedling growth. Higher TWI likely reduces this size-asymmetric competition for water,

Figure 4. Elasticity analysis showing the proportional change in life expectancy resulting from proportional changes in each of the vital rate parameters. (a) MLE_π represents the mean life expectancy of the smallest individuals (3–3.6 m in height), corresponding to individuals in the first 10% of bins with equal weighting. (b) Relative contributions of vital rate parameters to MLE_π. Parameters relating to topographic wetness index (TWI; green) and canopy density (purple) for each of the minor class and major class vital rate functions are shown. Letters inside the bars correspond to panels (c–f). Panels (c–f) show how the parameter perturbations from b impact the shape of the vital rate functions. Higher TWI generally increased life expectancy, driven primarily by higher survival probabilities in the minor class.

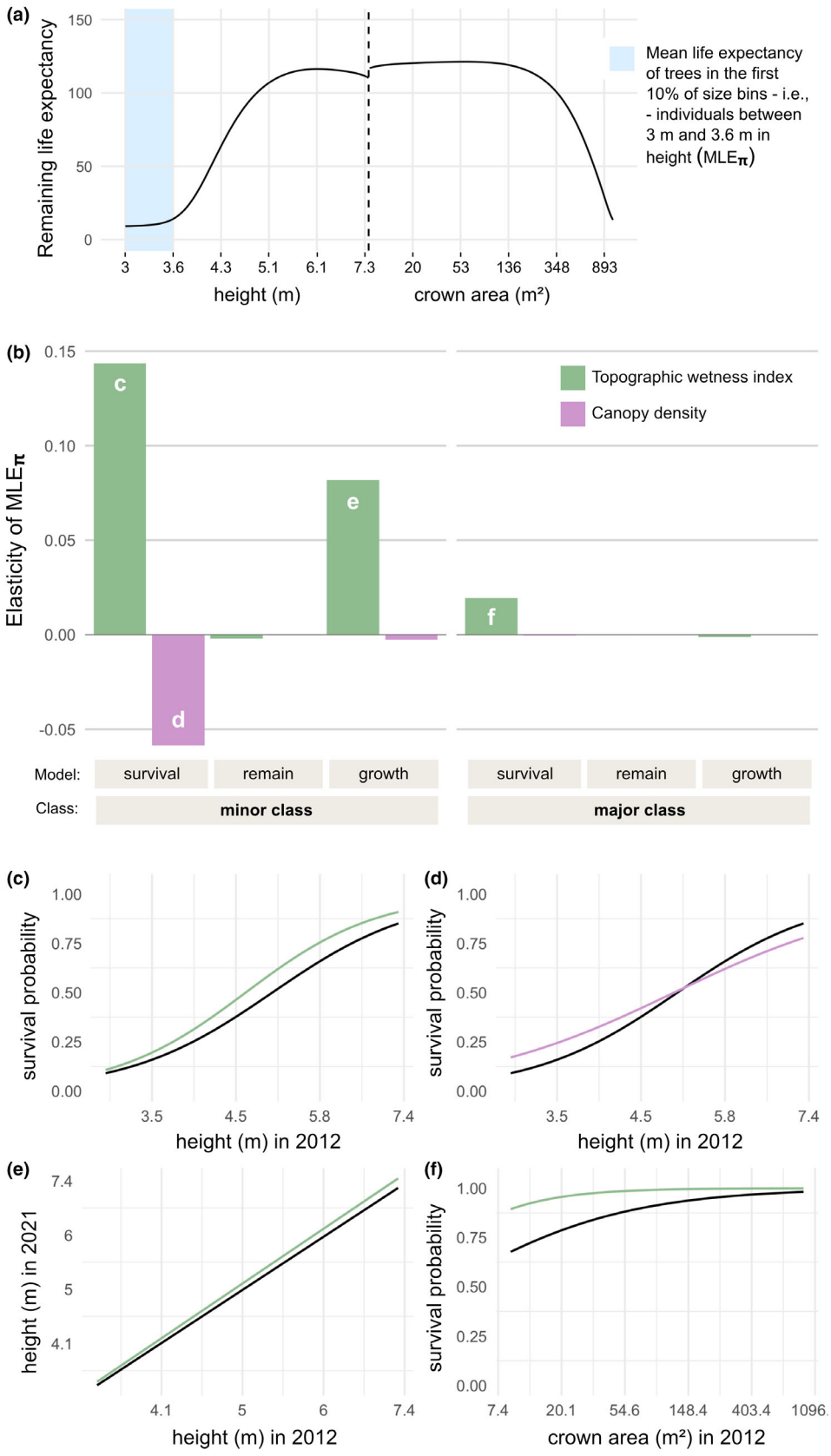

thereby improving small tree survival—the pathway through which life expectancy was most responsive in our elasticity analysis (Fig. 4).

Challenges and opportunities in complex forests

Tree segmentation algorithms now enable individual-level modelling over large areas with reasonable accuracy (Battison et al., 2024; Wang et al., 2016). In this study, we modelled survival and growth for over 42 000 trees—substantially exceeding the sample sizes used in most demographic models (Levin et al., 2022; Salguero-Gómez et al., 2015). The moderately sparse, open canopy of the eucalypt woodland lends itself to more accurate segmentation (Wang et al., 2016; Yang et al., 2019). The next major challenge is in applying these pipelines to more structurally complex systems, such as species-diverse forests with dense or multi-layered canopies. Algorithms calibrated to a wide variety of forest types or capable of handling diverse forest structures and data acquisition platforms (e.g. airborne, spaceborne, or ground-based) are promising solutions (e.g. deep-learning-based models; Henrich & van Delden, 2024; Wielgosz et al., 2024). However, achieving more generalizable and user-friendly tree segmentation methods—requiring minimal tuning for specific use cases—will depend on access to publicly available, high-quality, labelled forest datasets.

Species classification is essential for building species-specific models that account for varying life histories. While our study focused on a functionally similar eucalypt community, the species do differ in natural height ranges (*Eucalyptus salubris*: 9–13 m, *E. salmonophloia*: 10–20 m; Prober & Macfarlane, 2022) and may have different thresholds for switching from a dominance of height to crown growth. In more complex systems, hyperspectral remote sensing has been used for continent-scale tree species classification by leveraging species-specific spectral properties (Marconi et al., 2022). In a subtropical broadleaf forest, a combination of structural, spectral and textural features (derived from lidar, hyperspectral and RGB data) has been used to further enhance species classification accuracy (Qin et al., 2022). While such approaches are not always viable due to cost or data availability, the development of hyperspectral-lidar systems could make this type of sensor fusion more feasible (Fassnacht et al., 2016; Weinstein et al., 2024). Incorporating ground-based survey data will also be critical in addressing these challenges—for instance, by providing training data for species classification (Jia & Pang, 2023), or capturing important understory species that may be missed with airborne methods (Fassnacht et al., 2016).

Completing the life cycle

Capturing tree vital rates across their full life cycle remains a long-standing challenge in forest demography (Ohse et al., 2023; Ruiz-Benito et al., 2020). Here, we used repeat lidar to track individual-level survival/mortality, growth, and dieback processes. A key advantage of lidar is its ability to capture changes in 3D. Our results indicated distinct responses of small trees, which prioritize height growth, and large trees, which prioritize crown expansion, to biotic and abiotic factors such as canopy density and TWI. However, by excluding trees under 3 m to filter out small shrubs, we missed the smallest and youngest trees in the population, which likely have distinct patterns of growth and survival (Canham & Murphy, 2017; Metcalf et al., 2009). Future demographic studies should aim to better capture these early life stages and shifting growth patterns across a wide range of tree species. This could be achieved by integrating lidar (both airborne and terrestrial) with the extensive archive of field inventory data available through permanent forest plot networks that exist all over the world.

Mortality is particularly difficult to detect at the spatial scales and time intervals of most field surveys (McMahon et al., 2019). Here, we inferred mortality from threshold reductions in tree size or the disappearance of tree crowns, greatly improving our ability to detect tree deaths. However, lidar may miss mortality and dieback events in smaller trees, those obscured by dense canopies, or those at the early stages of decline. Our method may also misclassify severe dieback as mortality, even if trees later recover. Additional information, such as structural or spectral changes that precede death, could be used to improve mortality detection (Brodrick & Asner, 2017). Addressing these challenges is essential, as even small changes in mortality rates can have significant impacts on carbon cycling and ecosystem function (McMahon et al., 2019).

To model long-term population trajectories, including extinction risk and carbon cycling, it is necessary to complete the life cycle by modelling reproductive output or recruitment into a detectable size class (Ohse et al., 2023). In open canopy forests, lidar could help track these new recruits, offering a way to estimate the number of recruits produced by mature trees over time (Zambrano & Salguero-Gómez, 2014). To improve how recruits are attributed to mature trees, UAV or satellite imagery has been used to calculate flowering or fruiting probabilities at large spatial scales (Dixon et al., 2023), while field studies remain the best option for quantifying seed production, germination, and seedling survival probabilities (Ohse et al., 2023).

The future of forest demographic modelling

While this pipeline is not an out-of-the-box solution for all forest systems and contexts, it provides a foundation for scaling demographic models with under-utilized lidar data. Its value will grow with the availability of standardized, repeat lidar surveys and through integration with complementary data types. Beyond scale, remote sensing offers new opportunities for forest demography. Repeat surveys enable near-term forecasting, where predictions of demographic rates are updated with new observations (Itter & Finley, 2025), and inverse modelling, where vital rates are reconstructed from population-level time series (González et al., 2016). Together, these capabilities steer forest demography towards continuous, broad-scale modelling and prediction of population trajectories.

A key consideration is the choice of appropriate survey intervals. Short time intervals cannot adequately capture the growth of slow-growing trees, while long gaps between surveys risk missing events such as recruits that establish and die between observations. The ideal approach involves a greater number of surveys conducted at frequent intervals. Open data initiatives, such as NEON (Kampe et al., 2010), and more affordable platforms, like UAVs (Araujo et al., 2021), are making this more feasible. The additional context gained from more frequent surveys (e.g. leaf-on and leaf-off conditions) can further improve segmentation or species classification algorithms (Chen et al., 2022).

The comparability of lidar surveys is equally important. Differences in data acquisition (e.g. pulse density, flight elevation; Næsset, 2009), or in the way the data are processed (e.g. to produce CHMs) can introduce measurement error that compounds across time series. Errors in crown segmentation and cross-date matching can misrepresent true size changes or misclassify survival. Applying a standardized processing pipeline to lidar point clouds (Fischer et al., 2024) and propagating uncertainty through the modelling framework can help mitigate these issues.

Models that account for imperfect detection can improve inference by reducing bias. For example, multi-method occupancy models have been used to account for measurement error in tree mortality by combining information from field and remotely sensed measures (Barber et al., 2025). Bayesian state-space models similarly partition process uncertainty (e.g. changes in tree size or state) from measurement uncertainty (e.g. the ability of sensors to observe that state) (Pletcher & Shriver, 2025; Schultz et al., 2023). Both approaches reduce bias in vital rate estimation and carry observation uncertainty forward, rather than confounding it with the biological process (Louthan & Doak, 2018). In our pipeline, these modelling frameworks could estimate size- or context-dependent detectability (e.g. small or crowded crowns are harder to detect; Dalponte & Coomes, 2016) and propagate uncertainty end-to-end—from segmentation and crown matching through to vital rate modelling and IPM construction.

High-quality, standardized data from more frequent lidar surveys will greatly benefit our ability to build ecologically informative demographic models. While field surveys excel at species identification, understanding reproductive strategies, and capturing understory dynamics (Ohse et al., 2023), remote sensing offers the scalability needed to track forest responses to climate and disturbance at broad spatial and temporal scales. By leveraging the strengths of both approaches, we can build models that are better equipped to inform conservation and management strategies in a rapidly changing world.

Acknowledgements

We acknowledge and pay our respects to the First Nations people in the Great Western Woodlands on whose land this work was conducted. The project was funded by a Western Australian State NRM grant to the Ngadju Conservation Aboriginal Corporation and CSIRO and supported by the Australian Government through the TERN Great Western Woodlands Supersite and the TERN Landscapes platform. Airborne lidar from 2021 was collected by Landgate (Western Australia's land information authority) under the Capture WA program with additional support from the Western Australian Department of Biodiversity, Conservation and Attractions Goldfields Region office. AR was supported by the Oxford BBSRC Doctoral Training Partnership (BB/T008784/1). CMH and RSG were supported by a NERC Pushing the Frontiers grant to RSG (NE/X013766/1). CMH was additionally supported by a Marie Curie Fellowship (MSCA DensPopDy #10115386) with funding through UKRI (EP/Z002826/1). OGS was supported by the Oxford NERC Doctoral Training Partnership (NE/S007474/1). TJ was supported by a UK NERC Independent Research Fellowship (NE/S01537X/1) and by a UKRI Frontier Research grant (EP/Y003810/1) that also funded RB.

Author Contributions

Alice Rosen: Conceptualization; writing – original draft; writing – review and editing; visualization; methodology; validation; formal analysis. **Robin Battison:** Writing – review and editing; data curation; formal analysis; methodology. **Christina M. Hernández:** Writing – review and editing; methodology; formal analysis. **Oliver G. Spacey:** Writing – review and editing; methodology. **Jessica**

McLean: Writing – review and editing; methodology. **Suzanne M. Prober:** Writing – review and editing; methodology. **Samuel J. L. Gascoigne:** Writing – review and editing; methodology. **Sean McMahon:** Writing – review and editing; methodology. **Tommaso Jucker:** Conceptualization; writing – review and editing; supervision; methodology. **Roberto Salguero-Gómez:** Conceptualization; writing – review and editing; supervision; methodology.

Conflict of Interest Statement

No conflict of interest to declare.

Data Availability Statement

The 2012 lidar data used in this study are openly available through the TERN data portal (https://portal.tern.org.au). Data and code for tree segmentation and crown matching from the lidar data (Jucker, 2024) are publicly archived on Zenodo and can be accessed here: https://doi.org/10.5281/zenodo.13871110. All other data and code used for constructing the IPM and subsequent analyses are publicly archived on Zenodo, here: https://doi.org/10.5281/zenodo.15497708.

References

Araujo, R.F., Grubinger, S., Celes, C.H.S., Negrón-Juárez, R.I., Garcia, M., Dandois, J.P. et al. (2021) Strong temporal variation in treefall and branchfall rates in a tropical forest is related to extreme rainfall: Results from 5 years of monthly drone data for a 50 ha plot. *Biogeosciences*, **18**(24), 6517–6531. https://doi.org/10.5194/bg-18-6517-2021

Barber, C., Cruz, J., Graves, S.J., Bohlman, S.A., Zuidema, P.A., Asner, G.P. et al. (2025) Large, isolated trees have higher mortality than smaller trees in forest fragments across a tropical pastoral landscape. *Ecological Applications*, **35**(4), e70046. https://doi.org/10.1002/eap.70046

Bartholomew, D.C., Hayward, R., Burslem, D.F.R.P., Bittencourt, P.R.L., Chapman, D., Suis, M.A.F.B. et al. (2024) Bornean tropical forests recovering from logging at risk of regeneration failure. *Global Change Biology*, **30**(3), e17209. https://doi.org/10.1111/gcb.17209

Battison, R., Prober, S.M., Zdunic, K., Jackson, T.D., Fischer, F.J. & Jucker, T. (2024) Tracking tree demography and forest dynamics at scale using remote sensing. *New Phytologist*, **244**, 2251–2266. https://doi.org/10.1111/nph.20199

Beland, M., Parker, G., Sparrow, B., Harding, D., Chasmer, L., Phinn, S. et al. (2019) On promoting the use of lidar systems in forest ecosystem research. *Forest Ecology and Management*, **450**, 117484. https://doi.org/10.1016/j.foreco.2019.117484

Bennett, A.C., McDowell, N.G., Allen, C.D. & Anderson-Teixeira, K.J. (2015) Larger trees suffer most during drought in forests worldwide. *Nature Plants*, **1**(10), 15139. https://doi.org/10.1038/nplants.2015.139

Bogdziewicz, M., Chybicki, I., Szymkowiak, J., Ulaszewski, B., Burczyk, J., Szarek-Łukaszewska, G. et al. (2024) Masting and efficient production of seedlings: Balancing costs of variation through synchronised fruiting. *Ecology Letters*, **27**(9), e14514. https://doi.org/10.1111/ele.14514

Brodrick, P.G. & Asner, G.P. (2017) Remotely sensed predictors of conifer tree mortality during severe drought. *Environmental Research Letters*, **12**(11), 115013. https://doi.org/10.1088/1748-9326/aa8f55

Camarretta, N., Harrison, P.A., Bailey, T., Potts, B., Lucieer, A., Davidson, N. et al. (2020) Monitoring forest structure to guide adaptive management of forest restoration: A review of remote sensing approaches. *New Forests*, **51**(4), 573–596. https://doi.org/10.1007/s11056-019-09754-5

Canham, C.D. & Murphy, L. (2017) The demography of tree species response to climate: Sapling and canopy tree survival. *Ecosphere*, **8**(2), e01701. https://doi.org/10.1002/ecs2.1701

Chave, J., Réjou-Méchain, M., Búrquez, A., Chidumayo, E., Colgan, M.S., Delitti, W.B.C. et al. (2014) Improved allometric models to estimate the aboveground biomass of tropical trees. *Global Change Biology*, **20**(10), 3177–3190. https://doi.org/10.1111/gcb.12629

Chen, Q., Gao, T., Zhu, J., Wu, F., Li, X., Lu, D. et al. (2022) Individual tree segmentation and tree height estimation using leaf-off and leaf-on UAV-LiDAR data in dense deciduous forests. *Remote Sensing*, **14**(12), 2787. https://doi.org/10.3390/rs14122787

Clark, D.A. & Clark, D.B. (1992) Life history diversity of canopy and emergent trees in a neotropical rain Forest. *Ecological Monographs*, **62**(3), 315–344. https://doi.org/10.2307/2937114

Coulson, T. (2012) Integral projections models, their construction and use in posing hypotheses in ecology. *Oikos*, **121**(9), 1337–1350. https://doi.org/10.1111/j.1600-0706.2012.00035.x

CSIRO. (2022) *State of the climate 2022*. Melbourne, Australia: CSIRO & Bureau of Meteorology. https://www.csiro.au/en/research/environmental-impacts/climate-change/state-of-the-climate

Dalponte, M. & Coomes, D.A. (2016) Tree-centric mapping of forest carbon density from airborne laser scanning and hyperspectral data. *Methods in Ecology and Evolution*, **7**(10), 1236–1245. https://doi.org/10.1111/2041-210x.12575

Decocq, G., Regnault, P., Lenoir, J., Paccaut, F., di Menza, L., Delvoye, G. et al. (2023) Modelling plant community dynamics in changing forest ecosystems: A review. *Botany Letters*, **170**(4), 541–564. https://doi.org/10.1080/23818107.2023.2231045

Dixon, D.J., Duncan, J.M.A., Callow, J.N., Setterfield, S.A. & Pauli, N. (2023) Fire reduces eucalypt forest flowering

phenology at the landscape-scale. *Science of the Total Environment*, **894**, 164828. https://doi.org/10.1016/j.scitotenv.2023.164828

Doak, D.F., Gross, K. & Morris, W.F. (2005) Understanding and predicting the effects of sparse data on demographic analyses. *Ecology*, **86**(5), 1154–1163. https://doi.org/10.1890/04-0611

Dubayah, R., Armston, J., Healey, S.P., Bruening, J.M., Patterson, P.L., Kellner, J.R. et al. (2022) GEDI launches a new era of biomass inference from space. *Environmental Research Letters*, **17**(9), 095001. https://doi.org/10.1088/1748-9326/ac8694

Duncanson, L. & Dubayah, R. (2018) Monitoring individual tree-based change with airborne lidar. *Ecology and Evolution*, **8**(10), 5079–5089. https://doi.org/10.1002/ece3.4075

Easterling, M.R., Ellner, S.P. & Dixon, P.M. (2000) Size-specific sensitivity: Applying a new structured population model. *Ecology*, **81**(3), 694–708. https://doi.org/10.1890/0012-9658(2000)081[0694:sssaan]2.0.co;2

Fassnacht, F.E., Latifi, H., Stereńczak, K., Modzelewska, A., Lefsky, M., Waser, L.T. et al. (2016) Review of studies on tree species classification from remotely sensed data. *Remote Sensing of Environment*, **186** (For. Ecol. Manag. 260 10 2010), 64–87. https://doi.org/10.1016/j.rse.2016.08.013

Fischer, F.J., Jackson, T., Vincent, G. & Jucker, T. (2024) Robust characterisation of forest structure from airborne laser scanning—a systematic assessment and sample workflow for ecologists. *Methods in Ecology and Evolution*, **15**, 1873–1888. https://doi.org/10.1111/2041-210x.14416

Fischer, F. J. Morgan, B. Jackson, T. Chave, J. Coomes, D. Cushman, K. et al. (2025) The Global Canopy Atlas: Analysis-ready maps of 3D structure for the world's woody ecosystems bioRxiv https://doi.org/10.1101/2025.08.31.673375

Franceschini, T., Martin-Ducup, O. & Schneider, R. (2016) Allometric exponents as a tool to study the influence of climate on the trade-off between primary and secondary growth in major north-eastern American tree species. *Annals of Botany*, **117**(4), 551–563. https://doi.org/10.1093/aob/mcw003

González, E.J., Martorell, C. & Bolker, B.M. (2016) Inverse estimation of integral projection model parameters using time series of population-level data. *Methods in Ecology and Evolution*, **7**(2), 147–156. https://doi.org/10.1111/2041-210x.12519

Goodman, L.A. (1968) An elementary approach to the population projection-matrix, to the population reproductive value, and to related topics in the mathematical theory of population growth. *Demography*, **5**(1), 382–409. https://doi.org/10.1007/bf03208583

Gosper, C.R., Yates, C.J., Cook, G.D., Harvey, J.M., Liedloff, A.C., McCaw, W.L. et al. (2018) A conceptual model of vegetation dynamics for the unique obligate-seeder eucalypt woodlands of south-western Australia. *Austral Ecology*, **43**(6), 681–695. https://doi.org/10.1111/aec.12613

Griffith, A.B. (2017) Perturbation approaches for integral projection models. *Oikos*, **126**(12), 1675–1686. https://doi.org/10.1111/oik.04458

Henrich, J. & van Delden, J. (2024) Towards general deep-learning-boased tree instance segmentation models. arXiv. https://doi.org/10.48550/arxiv.2405.02061

Hijmans, R. J. (2024) terra: Spatial data analysis. https://CRAN.R-project.org/package=terra

Itter, M.S. & Finley, A.O. (2025) Toward improved uncertainty quantification in predictions of forest dynamics: A dynamical model of forest change. *Ecological Applications*, **35**(5), e70084. https://doi.org/10.1002/eap.70084

Jia, W. & Pang, Y. (2023) Tree species classification in an extensive forest area using airborne hyperspectral data under varying light conditions. *Journal of Forestry Research*, **34**(5), 1359–1377. https://doi.org/10.1007/s11676-022-01593-z

Jones, O.R., Barks, P., Stott, I., James, T.D., Levin, S., Petry, W.K. et al. (2022) Rcompadre and rage—two R packages to facilitate the use of the COMPADRE and COMADRE databases and calculation of life-history traits from matrix population models. *Methods in Ecology and Evolution*, **13**(4), 770–781. https://doi.org/10.1111/2041-210x.13792

Jucker, T., Fischer, F.J., Chave, J., Coomes, D.A., Caspersen, J., Ali, A. et al. (2022) Tallo: A global tree allometry and crown architecture database. *Global Change Biology*, **28**(17), 5254–5268. https://doi.org/10.1111/gcb.16302

Jucker, T., Gosper, C.R., Wiehl, G., Yeoh, P.B., Raisbeck-Brown, N., Fischer, F.J. et al. (2023) Using multi-platform LiDAR to guide the conservation of the world's largest temperate woodland. *Remote Sensing of Environment*, **296**, 113745. https://doi.org/10.1016/j.rse.2023.113745

Jucker, T. (2024). Data and R code supporting Battison et al. (2024) New Phytologist [Data set]. Zenodo https://doi.org/10.5281/zenodo.13871110.

Kampe, T.U., Johnson, B.R., Kuester, M. & Keller, M. (2010) NEON: The first continental-scale ecological observatory with airborne remote sensing of vegetation canopy biochemistry and structure. *Journal of Applied Remote Sensing*, **4**(1), 043510-043510–043524. https://doi.org/10.1117/1.3361375

Khosravipour, A., Skidmore, A.K., Isenburg, M., Wang, T. & Hussin, Y.A. (2014) Generating pit-free canopy height models from airborne lidar. *Photogrammetric Engineering & Remote Sensing*, **80**(9), 863–872. https://doi.org/10.14358/pers.80.9.863

King, D.A. (2011) Size-Related Changes in Tree Proportions and Their Potential Influence on the Course of Height Growth. In: Meinzer, F., Lachenbruch, B., Dawson, T. (eds) *Tree physiology*. Dordrecht: Springer Netherlands, vol **4**. pp. 165–191. https://doi.org/10.1007/978-94-007-1242-3_6

Kopecký, M., Macek, M. & Wild, J. (2021) Topographic wetness index calculation guidelines based on measured soil moisture and plant species composition. *Science of the Total*

Environment, **757**, 143785. https://doi.org/10.1016/j.scitotenv.2020.143785

Laurans, M., Munoz, F., Charles-Dominique, T., Heuret, P., Fortunel, C., Isnard, S. et al. (2024) Why incorporate plant architecture into trait-based ecology? *Trends in Ecology & Evolution*, **39**, 524–536. https://doi.org/10.1016/j.tree.2023.11.011

Levin, S.C., Evers, S., Potter, T., Guerrero, M.P., Childs, D.Z., Compagnoni, A. et al. (2022) Rpadrino: An R package to access and use PADRINO, an open access database of integral projection models. *Methods in Ecology and Evolution*, **13**(9), 1923–1929. https://doi.org/10.1111/2041-210x.13910

Lines, E.R., Fischer, F.J., Owen, H.J.F. & Jucker, T. (2022) The shape of trees: Reimagining forest ecology in three dimensions with remote sensing. *Journal of Ecology*, **110**, 1730–1745. https://doi.org/10.1111/1365-2745.13944

Louthan, A. & Doak, D. (2018) Measurement error of state variables creates substantial bias in results of demographic population models. *Ecology*, **99**(10), 2308–2317. https://doi.org/10.1002/ecy.2455

Ma, Q., Su, Y., Niu, C., Ma, Q., Hu, T., Luo, X. et al. (2023) Tree mortality during long-term droughts is lower in structurally complex forest stands. *Nature Communications*, **14**(1), 7467. https://doi.org/10.1038/s41467-023-43083-8

Marconi, S., Weinstein, B.G., Zou, S., Bohlman, S.A., Zare, A., Singh, A. et al. (2022) Continental-scale hyperspectral tree species classification in the United States National Ecological Observatory Network. *Remote Sensing of Environment*, **282**, 113264. https://doi.org/10.1016/j.rse.2022.113264

McDowell, N.G., Allen, C.D., Anderson-Teixeira, K., Aukema, B.H., Bond-Lamberty, B., Chini, L. et al. (2020) Pervasive shifts in forest dynamics in a changing world. *Science*, **368**(6494), eaaz9463. https://doi.org/10.1126/science.aaz9463

McMahon, S.M., Arellano, G. & Davies, S.J. (2019) The importance and challenges of detecting changes in forest mortality rates. *Ecosphere*, **10**(2), e02615. https://doi.org/10.1002/ecs2.2615

Merow, C., Dahlgren, J.P., Metcalf, C.J.E., Childs, D.Z., Evans, M.E.K., Jongejans, E. et al. (2014) Advancing population ecology with integral projection models: A practical guide. *Methods in Ecology and Evolution*, **5**(2), 99–110. https://doi.org/10.1111/2041-210x.12146

Metcalf, C.J.E., Horvitz, C.C., Tuljapurkar, S. & Clark, D.A. (2009) A time to grow and a time to die: A new way to analyze the dynamics of size, light, age, and death of tropical trees. *Ecology*, **90**(10), 2766–2778. https://doi.org/10.1890/08-1645.1

Metcalfe, P., Beven, K. & Freer, J. (2015) Dynamic TOPMODEL: A new implementation in R and its sensitivity to time and space steps. *Environmental Modelling & Software*, **72**, 155–172. https://doi.org/10.1016/j.envsoft.2015.06.010

Mielcarek, M., Stereńczak, K. & Khosravipour, A. (2018) Testing and evaluating different LiDAR-derived canopy height model generation methods for tree height estimation. *International Journal of Applied Earth Observation and Geoinformation*, **71**, 132–143. https://doi.org/10.1016/j.jag.2018.05.002

Næsset, E. (2009) Effects of different sensors, flying altitudes, and pulse repetition frequencies on forest canopy metrics and biophysical stand properties derived from small-footprint airborne laser data. *Remote Sensing of Environment*, **113**(1), 148–159. https://doi.org/10.1016/j.rse.2008.09.001

Needham, J.F., Johnson, D.J., Anderson-Teixeira, K.J., Bourg, N., Bunyavejchewin, S., Butt, N. et al. (2022) Demographic composition, not demographic diversity, predicts biomass and turnover across temperate and tropical forests. *Global Change Biology*, **28**(9), 2895–2909. https://doi.org/10.1111/gcb.16100

Needham, J., Merow, C., Chang-Yang, C.-H., Caswell, H. & McMahon, S.M. (2018) Inferring forest fate from demographic data: From vital rates to population dynamic models. *Proceedings of the Royal Society B: Biological Sciences*, **285**(1874), 20172050. https://doi.org/10.1098/rspb.2017.2050

Ohse, B., Compagnoni, A., Farrior, C.E., McMahon, S.M., Salguero-Gómez, R., Rüger, N. et al. (2023) Demographic synthesis for global tree species conservation. *Trends in Ecology & Evolution*, **38**(6), 579–590. https://doi.org/10.1016/j.tree.2023.01.013

Olsoy, P.J., Zaiats, A., Delparte, D.M., Germino, M.J., Richardson, B.A., Roser, A.V. et al. (2024) Demography with drones: Detecting growth and survival of shrubs with unoccupied aerial systems. *Restoration Ecology*, **32**(4), e14106. https://doi.org/10.1111/rec.14106

Peters, J.M.R., López, R., Nolf, M., Hutley, L.B., Wardlaw, T., Cernusak, L.A. et al. (2021) Living on the edge: A continental-scale assessment of forest vulnerability to drought. *Global Change Biology*, **27**(15), 3620–3641. https://doi.org/10.1111/gcb.15641

Pletcher, E. & Shriver, R.K. (2025) Density-dependent growth and dispersal can accurately forecast near-term range shifts in a dominant dryland tree species. *Journal of Ecology*, **113**, 3252–3264. https://doi.org/10.1111/1365-2745.70157

Pretzsch, H., Dauber, E. & Biber, P. (2013) Species-specific and ontogeny-related stem allometry of European Forest trees: Evidence from extensive stem analyses. *Forest Science*, **59**(3), 290–302. https://doi.org/10.5849/forsci.11-102

Prober, S. M. & Macfarlane, C. K. (2022) Great Western Woodlands Vegetation Structure Data, 2013. Version 1.0. Terrestrial Ecosystem Research Network (Dataset). https://doi.org/10.25901/4d24-9q64.

Prober, S.M., Thiele, K.R., Rundel, P.W., Yates, C.J., Berry, S.L., Byrne, M. et al. (2012) Facilitating adaptation of biodiversity to climate change: A conceptual framework applied to the world's largest Mediterranean-climate woodland. *Climatic Change*, **110**(1–2), 227–248. https://doi.org/10.1007/s10584-011-0092-y

Qin, H., Zhou, W., Yao, Y. & Wang, W. (2022) Individual tree segmentation and tree species classification in subtropical broadleaf forests using UAV-based LiDAR, hyperspectral, and ultrahigh-resolution RGB data. *Remote Sensing of Environment*, **280**, 113143. https://doi.org/10.1016/j.rse.2022.113143

R Core Team. (2021) *R: A language and environment for statistical computing*. Vienna, Austria: R Foundation for Statistical Computing. https://www.R-project.org/

Ramula, S., Rees, M. & Buckley, Y.M. (2009) Integral projection models perform better for small demographic data sets than matrix population models: A case study of two perennial herbs. *Journal of Applied Ecology*, **46**(5), 1048–1053. https://doi.org/10.1111/j.1365-2664.2009.01706.x

Ruiz-Benito, P., Vacchiano, G., Lines, E.R., Reyer, C.P.O., Ratcliffe, S., Morin, X. et al. (2020) Available and missing data to model impact of climate change on European forests. *Ecological Modelling*, **416**, 108870. https://doi.org/10.1016/j.ecolmodel.2019.108870

Salguero-Gómez, R., Jones, O.R., Archer, C.R., Buckley, Y.M., Che-Castaldo, J., Caswell, H. et al. (2015) The compadre Plant Matrix Database: An open online repository for plant demography. *Journal of Ecology*, **103**(1), 202–218. https://doi.org/10.1111/1365-2745.12334

Salguero-Gómez, R., Jones, O.R., Jongejans, E., Blomberg, S.P., Hodgson, D.J., Mbeau-Ache, C. et al. (2016) Fast–slow continuum and reproductive strategies structure plant life-history variation worldwide. *Proceedings of the National Academy of Sciences of the United States of America*, **113**(1), 230–235. https://doi.org/10.1073/pnas.1506215112

Schultz, E.L., Filippelli, S.K., Vogeler, J.C. & Shriver, R.K. (2023) Density-dependent dynamics help explain the simultaneous expansion and decline of woodlands in the western US. *Forest Ecology and Management*, **546**, 121359. https://doi.org/10.1016/j.foreco.2023.121359

Seidl, R. & Turner, M.G. (2022) Post-disturbance reorganization of forest ecosystems in a changing world. *Proceedings of the National Academy of Sciences of the United States of America*, **119**(28), e2202190119. https://doi.org/10.1073/pnas.2202190119

Trouillier, M., van der Maaten-Theunissen, M., Scharnweber, T., Würth, D., Burger, A., Schnittler, M. et al. (2019) Size matters—a comparison of three methods to assess age- and size-dependent climate sensitivity of trees. *Trees*, **33**(1), 183–192. https://doi.org/10.1007/s00468-018-1767-z

Vanderwel, M.C., Lopez, E.L., Sprott, A.H., Khayyatkhoshnevis, P. & Shovon, T.A. (2020) Using aerial canopy data from UAVs to measure the effects of neighbourhood competition on individual tree growth. *Forest Ecology and Management*, **461**, 117949. https://doi.org/10.1016/j.foreco.2020.117949

Wang, Y., Hyyppa, J., Liang, X., Kaartinen, H., Yu, X., Lindberg, E. et al. (2016) International benchmarking of the individual tree detection methods for modeling 3-D canopy structure for silviculture and Forest ecology using airborne laser scanning. *IEEE Transactions on Geoscience and Remote Sensing*, **54**(9), 5011–5027. https://doi.org/10.1109/tgrs.2016.2543225

Watson, A., Judd, S., Watson, J., Lam, A. & Mackenzie, D. (2008) *The extraordinary nature of the great Western woodlands*. Perth, WA: The Wilderness Society.

Weinstein, B.G., Marconi, S., Zare, A., Bohlman, S.A., Singh, A., Graves, S.J. et al. (2024) Individual canopy tree species maps for the National Ecological Observatory Network. *PLoS Biology*, **22**(7), e3002700. https://doi.org/10.1371/journal.pbio.3002700

Wielgosz, M., Puliti, S., Xiang, B., Schindler, K. & Astrup, R. (2024) SegmentAnyTree: A sensor and platform agnostic deep learning model for tree segmentation using laser scanning data. *Remote Sensing of Environment*, **313**, 114367. https://doi.org/10.1016/j.rse.2024.114367

Yang, Q., Su, Y., Jin, S., Kelly, M., Hu, T., Ma, Q. et al. (2019) The influence of vegetation characteristics on individual tree segmentation methods with airborne LiDAR data. *Remote Sensing*, **11**(23), 2880. https://doi.org/10.3390/rs11232880

Yates, C.J., Hobbs, R.J. & Atkins, L. (2000) Establishment of perennial shrub and tree species in degraded Eucalyptus salmonophloia (Salmon gum) remnant woodlands: Effects of restoration treatments. *Restoration Ecology*, **8**(2), 135–143. https://doi.org/10.1046/j.1526-100x.2000.80020.x

Zambrano, J. & Salguero-Gómez, R. (2014) Forest fragmentation alters the population dynamics of a late-successional tropical tree. *Biotropica*, **46**(5), 556–564. https://doi.org/10.1111/btp.12144

Zhang, B., Fischer, F.J., Prober, S.M., Yeoh, P.B., Gosper, C.R., Zdunic, K. et al. (2024) Robust retrieval of forest canopy structural attributes using multi-platform airborne LiDAR. *Remote Sensing in Ecology and Conservation*, **10**, 725–742. https://doi.org/10.1002/rse2.398

Zhao, D., Borders, B., Wilson, M. & Rathbun, S.L. (2006) Modeling neighborhood effects on the growth and survival of individual trees in a natural temperate species-rich forest. *Ecological Modelling*, **196**(1–2), 90–102. https://doi.org/10.1016/j.ecolmodel.2006.02.002

Supporting Information

Additional supporting information may be found online in the Supporting Information section at the end of the article.

Data S1. Supplementary Figures and Tables.